Bi-allelic Mutations in the Mitochondrial Ribosomal Protein MRPS2 Cause Sensorineural Hearing Loss, Hypoglycemia, and Multiple OXPHOS Complex Deficiencies

Thatjana Gardeitchik,[1,2,14] Miski Mohamed,[1,14] Benedetta Ruzzenente,[3,14] Daniela Karall,[4,15] Sergio Guerrero-Castillo,[1,5,6,15] Daisy Dalloyaux,[1] Mariël van den Brand,[1,5] Sanne van Kraaij,[1,6] Ellyze van Asbeck,[1] Zahra Assouline,[7] Marlene Rio,[7] Pascale de Lonlay,[13] Sabine Scholl-Buergi,[4] David F.G.J. Wolthuis,[1] Alexander Hoischen,[2] Richard J. Rodenburg,[5,6] Wolfgang Sperl,[4] Zsolt Urban,[8] Ulrich Brandt,[1,5,6] Johannes A. Mayr,[9] Sunnie Wong,[10] Arjan P.M. de Brouwer,[2,11] Leo Nijtmans,[1,5] Arnold Munnich,[3,7] Agnès Rötig,[3] Ron A. Wevers,[6,16] Metodi D. Metodiev,[3,16,*] and Eva Morava[12,16,*]

Biogenesis of the mitochondrial oxidative phosphorylation system, which produces the bulk of ATP for almost all eukaryotic cells, depends on the translation of 13 mtDNA-encoded polypeptides by mitochondria-specific ribosomes in the mitochondrial matrix. These mitoribosomes are dual-origin ribonucleoprotein complexes, which contain mtDNA-encoded rRNAs and tRNAs and ~80 nucleus-encoded proteins. An increasing number of gene mutations that impair mitoribosomal function and result in multiple OXPHOS deficiencies are being linked to human mitochondrial diseases. Using exome sequencing in two unrelated subjects presenting with sensorineural hearing impairment, mild developmental delay, hypoglycemia, and a combined OXPHOS deficiency, we identified mutations in the gene encoding the mitochondrial ribosomal protein S2, which has not previously been implicated in disease. Characterization of subjects' fibroblasts revealed a decrease in the steady-state amounts of mutant MRPS2, and this decrease was shown by complexome profiling to prevent the assembly of the small mitoribosomal subunit. In turn, mitochondrial translation was inhibited, resulting in a combined OXPHOS deficiency detectable in subjects' muscle and liver biopsies as well as in cultured skin fibroblasts. Reintroduction of wild-type MRPS2 restored mitochondrial translation and OXPHOS assembly. The combination of lactic acidemia, hypoglycemia, and sensorineural hearing loss, especially in the presence of a combined OXPHOS deficiency, should raise suspicion for a ribosomal-subunit-related mitochondrial defect, and clinical recognition could allow for a targeted diagnostic approach. The identification of *MRPS2* as an additional gene related to mitochondrial disease further expands the genetic and phenotypic spectra of OXPHOS deficiencies caused by impaired mitochondrial translation.

Mitochondria are essential organelles that harbor the oxidative phosphorylation system (OXPHOS), an ATP-producing system encompassing five multi-subunit enzymatic complexes whose biogenesis is strictly dependent on the coordinated expression of genes encoded by nuclear and mitochondrial DNA (mtDNA). mtDNA encodes 13 subunits that are essential structural components of OXPHOS complexes I, III, IV, and V, in addition to encoding two rRNAs (16S and 12S) and 22 tRNAs required for the translation of the subunits.[1] Mitochondrial translation is executed by a dedicated translation machinery that includes many regulatory factors and a mitochondrial-specific ribosome composed of two subunits: the 28S (mt-SSU) and 39S (mt-LSU) ribosomal subunits. These subunits are large ribonucleoprotein complexes containing around 80 nuclear-encoded structural mitoribosomal proteins (MRPs) and mt-DNA-encoded RNAs: 12S rRNA in the mt-SSU and 16S rRNA, in addition to either mt-tRNA^{Val} or mt-tRNA^{Phe}, in the mt-LSU subunit.[2–5] The three-dimensional structures of the mammalian[3,6,7] and human[2] mitoribosomes have only been elucidated recently.

Considering the many factors involved in this process, it is not surprising that an increasing number of gene mutations cause defective mitochondrial translation and are linked to mitochondrial disease.[1,3] Mitochondrial translation defects usually result in a combined OXPHOS complex deficiency, leading to disorders with severe multisystem involvement and often an early lethal outcome. To date, mutations in eight mitoribosomal protein-encoding genes—*MRPS7* (MIM: 611974), *MRPS16* (MIM: 609204),

[1]Department of Pediatrics, Radboud University Medical Center, 6500 HB Nijmegen, the Netherlands; [2]Department of Human Genetics, Radboud University Medical Center, 6500 HB Nijmegen, the Netherlands; [3]INSERM U1163, Université Paris Descartes-Sorbonne Paris Cité, Institut Imagine, 75015 Paris, France; [4]Clinic for Pediatrics, Inherited Metabolic Disorders, Medical University of Innsbruck, 6020 Innsbruck, Austria; [5]Radboud Center for Mitochondrial Medicine, Department of Pediatrics, Medical Center, 6500 HB Nijmegen, the Netherlands; [6]Translational Metabolic Laboratory, Department of Laboratory Medicine, Radboud University Medical Center, 6500 HB Nijmegen, the Netherlands; [7]Departments of Pediatrics, Neurology, and Genetics, Hôpital Necker-Enfants-Malades, 75015 Paris, France; [8]Department of Human Genetics, University of Pittsburgh Graduate School of Public Health, Pittsburgh, PA 15261, USA; [9]Department of Pediatrics, Paracelsus Medical University, Salzburg, Austria; [10]Hayward Genetics Center, Tulane University, LA 70112, USA; [11]Donders Institute for Brain, Cognition and Behaviour, Medical Center, 6500 HB Nijmegen, the Netherlands; [12]Department of Clinical Genomics, Mayo Clinic, Rochester, MN 55905, USA; [13]Reference Center for Inherited Metabolic Diseases, Hôpital Necker-Enfants-Malades, Assistance Publique – Hôpitaux de Paris, Université Paris Descartes, Institut Imagine, 75015 Paris, France
[14]These authors contributed equally to this work
[15]These authors contributed equally to this work
[16]These authors contributed equally to this work
*Correspondence: metodi.metodiev@inserm.fr (M.D.M.), emoravakozicz@tulane.edu (E.M.)
https://doi.org/10.1016/j.ajhg.2018.02.012.

MRPS22 (MIM: 605810), *MRPS23* (MIM: 611985), and *MRPS34* (MIM: 611994) from the mt-SSU and *MRPL3* (MIM: 607118), *MRPL12* (MIM: 602375), and *MRPL44* (MIM: 611849) from the mt-LSU—have been linked to mitochondrial disease in a total of 22 subjects (summarized in Table 1).

Most subjects presented in the neonatal period, and about one-third of the subjects died before the age of 1 year. However, besides the common feature of severe lactic acidosis, these disorders show a large variety in clinical presentation. Some have specific clinical features such as early-onset cardiomyopathy,[8–10] developmental abnormalities,[10–12] corpus callosum agenesis,[13] hypoglycemia,[14] Leigh syndrome,[12] or short stature and dysmorphic features.[9,12,13] Wrinkled or redundant skin has been observed in mitochondrial translation defects caused by mutations in *MRPS22*[9,13] and *MRPS16*.[11]

Here, we report two unrelated subjects presenting with sensorineural hearing impairment, developmental delay, hypoglycemia, lactic acidemia, and a combined OXPHOS deficiency. Using exome sequencing, we identified bi-allelic mutations in *MRPS2* (MIM: 611971), which encodes the mitochondrial ribosomal protein S2 and has not been implicated in disease until now.

Our study adhered to the Declaration of Helsinki and was approved by the institutional review boards at each research site. Written informed consent was obtained from the parents of the subjects.

Subject 1, a girl, was born at term after an uneventful pregnancy as the third child of non-consanguineous healthy parents of Austrian origin (Figure 1). Birth parameters were within normal limits. She had minor dysmorphic features, including low-set ears and slightly up-slanting palpebral fissures. Skin wrinkling, most pronounced on the abdomen and hands, was apparent from birth. During the first year of life she developed a failure to thrive. She had a psychomotor developmental delay in which the motor delay was most pronounced. She had an intermittent divergent strabismus of the left eye. At the age of 3 years, she had developed progressive sensorineural hearing loss, which required the use of a hearing aid and was corrected with bilateral cochlea implants. After this correction, both her speech and development improved markedly. Her last formal developmental assessment at the age of 5 years and 10 months showed an average developmental state of 2 years and 6 months of age. A cerebral MRI at the age of 3 years did not reveal any structural anomalies. She was prone to developing hypoglycemia. Biochemical evaluation revealed elevated liver enzymes (3- to 4-fold elevation in aspartate-amino transferase and alanine-amino transferase, repetitive elevated lactate levels (>8 mmol/L; reference values < 2 mmol/L), elevated serum alanine (up to 850 μmol/L; reference values = 99–350 μmol/L), and increased excretion of Krebs cycle intermediates (2-oxoglutaric acid between 50–220 μmol/mmol creatinine; reference values = 0–50 μmol/mmol creatinine and trace elevation of succinic acid). Glycosylation screening (transferrin and apolipoprotein-CIII isoelectric focusing) was unremarkable. Normal serum creatine kinase (CK) concentrations were found. Measurements of OXPHOS complex activities in liver, muscle, and fibroblasts showed a decrease in multiple enzyme complexes (Table 2).

Subject 2, a boy, presented with fasting hypoglycemia at the age of 6 years. He was the first child of healthy unrelated parents of Tunisian origin and was born at term after an uneventful pregnancy. Birth parameters were within normal limits. Medical history was marked by several acute episodes of hypoglycemia after an overnight or a 12-hr fasting since the age of 18 months, especially when these episodes coincided with illness and poor oral intake, which associated with lactic acidosis. He could walk at 22 months. Speech development was delayed as a result of severe sensorineural deafness at the age of 2 years, necessitating the use of a hearing aid. Speech development improved after the hearing loss was corrected. At the age of 11 years he had a normal physical appearance, with normal growth parameters, but a moderate intellectual disability, frequent headache episodes, and muscular weakness of the lower limbs. He suffered from exercise intolerance marked by myalgia after walking. His brain MRI was normal. Metabolic investigations showed repetitive mildly increased lactate levels in plasma (2.2–3.8 mmol/L; reference values < 2 mmol/L) and urine (292 μmol/mmol creatinine; reference values = 25–100 μmol/mmol creatinine). A clinical fasting test showed hypoglycemia with hyperlactatemia (5 mmol/L) and slightly increased excretion of 2-oxoglutarate (37 μmol/mmol creatinine; control range < 27 μmol/mmol creatinine) in urine. Measurements of OXPHOS complex activities showed a decrease in multiple complexes in liver and fibroblasts and a complex IV deficiency in muscle. This subject had two unaffected siblings. A third sibling died during pregnancy (Figure 2B). The cause of her death is unknown, so it is unclear whether it is related to mitochondrial disease.

Exome sequencing was performed to identify pathogenic variants underlying the disease in both subjects (for methods, see Supplemental Data). For subject 1, a series of filter steps, comparable to those described by Gilissen et al.,[15] was applied to the variant data for the creation of a candidate gene list. Non-genic, intronic (except for splice sites), synonymous changes and common variants were excluded by comparison with dbSNPv132 and our in-house variant database (cutoff > 1%). Variants were further prioritized on the basis of PhyloP scores (cutoff > 3) as well as molecular pathways and segregation analysis. This resulted in the identification of a single candidate gene, mitochondrial ribosomal protein S2 (*MRPS2*; GenBank: NM_016034.3), carrying two heterozygous sequence variants, c.328C>T (p.Arg110Cys) and c.340G>A (p.Asp114Asn) (Figure 2A). Segregation analysis confirmed that both parents are heterozygous for one of these variants. One healthy sibling was homozygous for both wild-type alleles, whereas the second was heterozygous for the c.328C>T variant (data not shown).

Table 1. Overview of the Clinical Features of Subjects Carrying Mutations in Mitoribosomal Subunits

	MRPS2	*MRPS2*	*MRPS7*	*MRPS16*	*MRPS22*	*MRPS22*	*MRPS22*	*MRPS23*	*MPRS34*	*MRPL3*	*MRPL12*	*MRPL44*	*MRPL44*
Reference	**this article (S1)**	**this article (S2)**	**Menezes et al.[16]**	**Miller et al.[11]**	**Saada et al.[13]**	**Smits et al.[9]**	**Baertling et al.[19]**	**Kohda et al.[14]**	**Lake et al.[12]**	**Galmiche et al.[8]**	**Serre et al.[33]**	**Distelmaier et al.[10]**	**Distelmaier et al.[10]**
Number of subjects	1	1	2 siblings	1	3 siblings	1	1	1	6	4 siblings	1	1	1
Dysmorphic features	+	−	−	+	NR	+	NR	NR	+	−	+	−	−
Cardiac involvement	−	−	−	+	+	+	+	NR	−	+	NR	+	+
Hypotonia	+	+	NR	+	+	+	NR	NR	+	NR	+	+	NR
Skin involvement	+	−	−	redundant skin of the neck	−	redundant skin of the neck	−	NR	−	−	NR	−	−
Structural brain abnormalities	−	−	NR	+	NR	+	+	NR	+	+	+	NR	NR
Hearing impairment	+	+	++	NR	NR	−	NR	NR	−	NR	NR	NR	NR
Developmental delay	+/−	+	−	NR	NR	++	NR	NR	+	++	+	−	+/−
Growth delay	FTT	−	FTT	SGA	NR	NR	+	NR	+	FTT	SGA, FTT	NR	NR
Increased lactate levels	++	+	+	+	++	+	++	NR	+	+	+	+	+
Combined OXPHOS deficiency	+	+	+	+	+	+	+	+	+	+	+	+	+
Hypoglycemia	+	+	NR	NR	NR	NR	NR	+	NR	NR	NR	NR	NR
Age of presentation	infantile	infantile	infantile	neonatal	neonatal	neonatal	neonatal	infantile	neonatal or infantile	infantile	neonatal	infantile	neonatal
Age of death (or age at last follow up)	alive at 11 years	alive at 11 years	14 years; alive at 17 years	3 days	2–22 days	alive at 5 years	3 days	alive at 1 year and 6 months	range: dead at 8.5 months to alive at 17 years	two died at 15 and 17 months; two are alive at 3 years	2 years	alive at 8 years	alive at 26 years

Abbreviations are as follows: −, not present; +/−, mildly affected; +, present; ++, severely affected; NR, not reported; FTT, failure to thrive; SGA, small for gestational age.

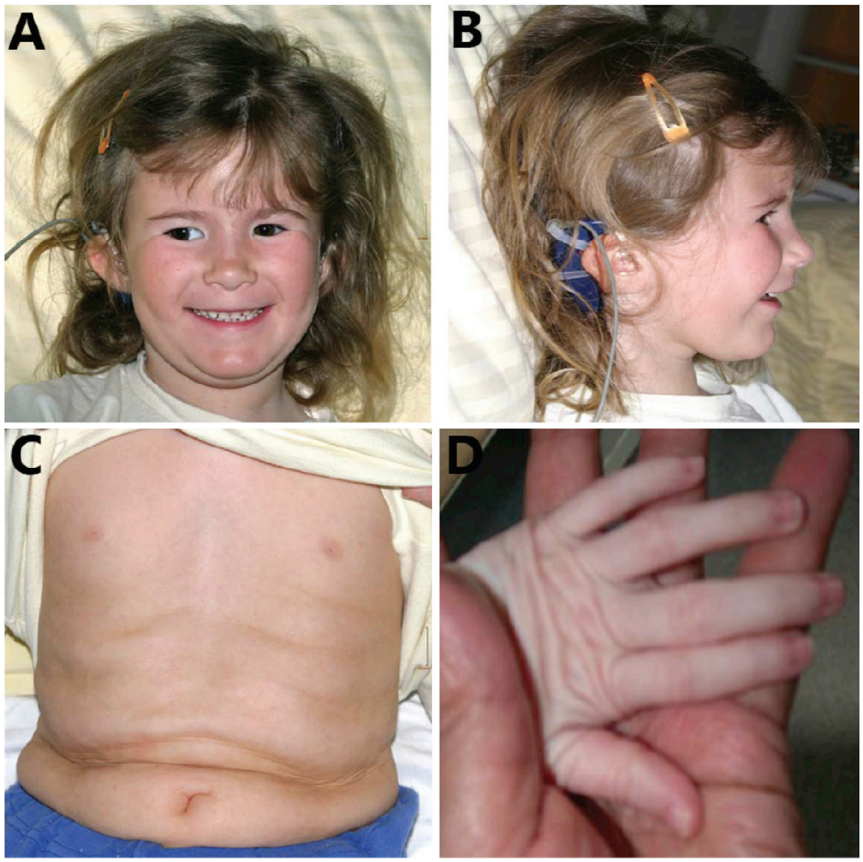

Figure 1. Clinical Characteristics of Subject 1 at the Age of 5 Years
Clinical features include (A) slightly upslanting palpebral fissures and left-eye strabismus, (B) low-set ears, and redundant skin on the (C) abdomen and (D) hands.

For subject 2, the pathogenic variant was selected according to similar criteria: exclusion of known SNPs reported with a frequency > 0.1% in dbSNP, 1000 Genomes, Exome Variant Server, or our in-house database; exclusion of non-coding variants; and selection of variants that were predicted to be possibly damaging by PolyPhen and SIFT. This filtering identified a homozygous variation (c.413G>A [p.Arg138His]) in only one gene: *MRPS2*, which encodes a known mitochondrial protein. Segregation analysis confirmed that both parents are heterozygous for this variant (Figure 2B).

All identified variants affect highly conserved amino acids (Figure 2C) and were predicted to be pathogenic by at least two of the three *in silico* prediction programs that were used. These variants are reported in the GnomAD database only as heterozygous variants with very low minor allele frequencies (Table S1).

Given that MRPS2 is a mitochondrial ribosomal protein, we proceeded to characterize the effects of the identified variants on mitochondrial physiology by using fibroblasts obtained from skin biopsies of both subjects (S1 and S2). A previously characterized fibroblast cell line (designated S3) carrying disease-causing mutations in *MRPS22* was used as a positive control for mitoribosomal dysfunction.[9]

SDS-PAGE analysis of mitochondrial extracts (for methods, see Supplemental Data) from these fibroblasts showed decreased steady-state amounts of the protein MRPS2 in both S1 and S2 fibroblasts (Figure 3A). Similarly, the mt-SSU proteins MRPS5, MRPS18B, and MRPS28 were less abundant in subject fibroblasts. Amounts of the mt-LSU proteins MRPL37 and MRPL44 remained unchanged. Stability of newly imported mitoribosomal proteins and nascent 12S rRNA depends on their coordinated assembly into ribonucleoprotein complexes. Loss of individual MRPS proteins has been previously shown to result in decreased 12S rRNA steady-state abundance.[9,11,13,16] Consistent with this, steady-state abundance of 12S rRNA, but not that of 16S rRNA, was specifically decreased in S1 and S2 fibroblasts; a similar decrease was

Table 2. OXPHOS Complex Enzyme Activities in Muscle, Liver, and Fibroblasts

	Complex Activity in Muscle		Complex Activity in Liver		Complex Activity in Fibroblasts	
	Subject 1	**Subject 2**	**Subject 1**	**Subject 2**	**Subject 1**	**Subject 2**
Complex I	0. 14 (0.14–0.35)	0.20 (0.13–0.29)	0.02 ↓ (0.24; 0.59)	0.02 ↓ (0.35–0.50)	0.04 (0.04–0.12)	0.16 (0.13–0.26)
Complex II	0.22 ↓ (0.23–0.41)	0.19 ↑(0.09–0.15)	1.43 (0.85; 1.80)	0.9 ↓ (1.70–2.50)	0.23 (0.18–0.43)	0.36 ↑(0.25–0.34)
Complex III	0.81 ↓ (1.45–3.76)	NP	0.34 ↓ (2.18; 3.18)	0.23 ↓ (1.00–1.40)	0.96 (0.72–2.23)	2.16 ↓ (2.23–2.98)
Complex IV	0.51 ↓ (0.82–2.04)	0.42 ↓ (0.45–0.75)	0.09 ↓ (1.44; 1.66)	0.12 ↓ (1.00–1.40)	0.24 ↓ (0.90–1.79)	0.99 ↓ (1.14–1.54)
Complex V	0.67 (0.42–1.26)	NP	0.43 (0.31; 1.21)	NP	0.39 (0.39–0.79)	0.48 (0.23–0.33)

Laboratory reference values were available for muscle, fibroblasts, and liver and are shown in parentheses. Complex activities in liver for subject 1 are compared with those in two control samples that were used in the same experiment. These values are reported in parentheses. The following abbreviation is used: NP, not performed.

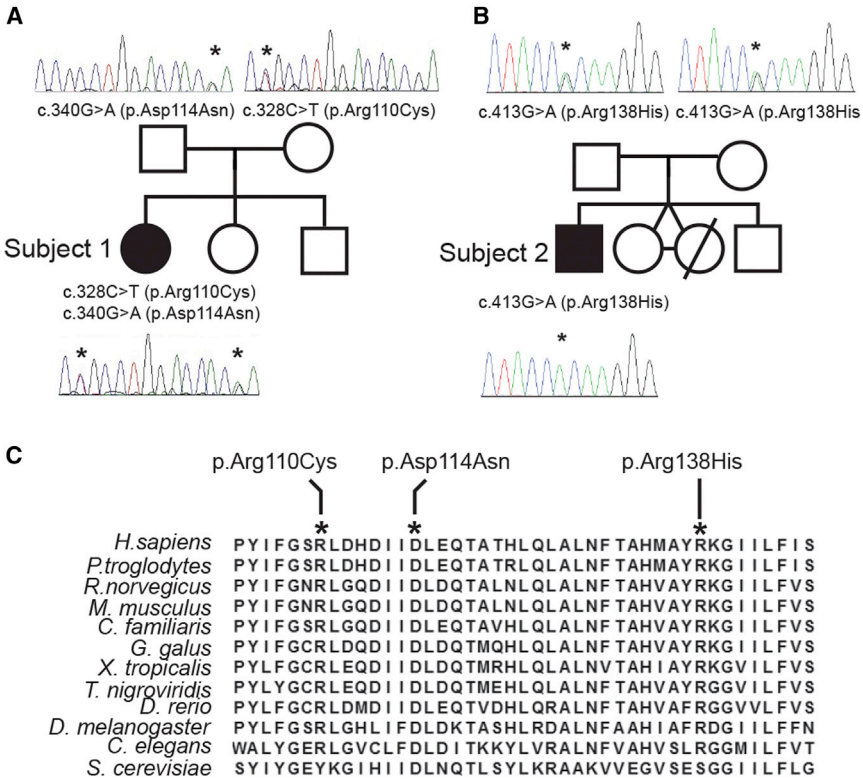

Figure 2. *MRPS2* Mutation Analysis and Evolutionary Conservation of the Affected Amino Acid Residues

(A and B) Pedigree and sequencing chromatograms for (A) S1 and (B) S2 and their families, depicting the segregation of the identified recessive mutations.

(C) Interspecies alignment of the MRPS2 region containing the amino acid residues altered (depicted in bold and italics) in S1 and S2.

seen in S3 fibroblasts (Figure 3B) on northern blot analysis (for methods, see Supplemental Data).

To further characterize the detrimental effects of *MRPS2* mutations on mitoribosomal biogenesis, we analyzed the assembly and abundance of mt-SSU and mt-LSU particles with complexome profiling of mitochondrial extracts from control, S1, and S3 fibroblasts (for methods, see Supplemental Data). Complexome profiling enables the investigation of the abundance and composition of macromolecular protein complexes.[17] Fully assembled mt-SSU particles were hardly detectable in both S1 and S3 fibroblasts, whereas mt-LSU particles were assembled at a normal level (Figure 4). A previously reported, ~300 kDa mt-SSU subassembly containing MRPS16, MRPS17, MRPS18B, MRPS22, MRPS26, MRPS27, and MRPS34[18] was detectable in control fibroblasts and was also preserved, albeit at reduced levels, in S1 mitochondria, suggesting that MRPS2 is unlikely to function in the early assembly pathway. Cumulatively, these data indicate that the identified mutations in *MRPS2* destabilize the protein and thereby impair mt-SSU assembly in subjects 1 and 2.

Decreased mt-SSU assembly and the resulting lack of functional mitoribosomes invariably lead to an inhibition of mitochondrial translation and multiple OXPHOS deficiencies. Indeed, *in vitro* pulse labeling of mitochondrial translation products with radiolabeled methionine and cysteine revealed a profound and generalized translation defect of mtDNA-encoded polypeptides in both S1 and S2 fibroblasts, as well as in the MRPS22-deficient fibroblasts (Figure 5A; for methods, see Supplemental Data).

In line with this impaired translation, BN-PAGE analysis of OXPHOS complex assembly revealed decreased amounts of fully assembled OXPHOS complexes I and IV but not of complex III and the exclusively nucleus-encoded complex II (Figure 5B; for methods, see Supplemental Data). Although no differences in abundance of fully assembled complex V were seen in S1 and S2 fibroblasts, BN-PAGE analysis revealed the presence of subcomplexes of complex V, which were absent in the controls (Figure 5B). Interaction profiles of the different OXPHOS complexes extracted from the complexome profiling data for S1 consistently confirmed a decrease in the abundance of fully assembled complex I and IV. Furthermore, complexome profiling showed an accumulation of complex I and complex V subassemblies at lower molecular masses in the S1 fibroblasts than in the control cells (Figure S1).

To demonstrate the disease-causing nature of *MRPS2* mutations, we carried out functional complementation experiments by generating control, S1, and S2 cell lines stably expressing either green fluorescent protein (GFP) as a negative control or wild-type MRPS2 (for methods, see Supplemental Data). SDS-PAGE analysis and immunoblotting of whole-cell extracts from these cell lines revealed that despite the markedly different abundance of MRPS2 (Figure 6A), the amounts of steady-state MRPS5 and MRPS18B were higher in S1 and S2 cells complemented with MRPS2 than in the same cells expressing GFP. Likewise, the OXPHOS proteins NDUFB8 and NDUFA13 from complex I as well as COXI and COXIV from complex IV accumulated in MRPS2-complemented fibroblasts, suggesting restoration of OXPHOS biogenesis. Consistent with these observations, mitochondrial translation was partially restored in both subject cell lines complemented with wild-type MRPS2 (Figure 6B), as was the assembly of OXPHOS complexes I and IV (Figure 6C). We also noted fewer complex V subassemblies in MRPS2-expressing subjects' fibroblasts than in the negative control cells. Overexpression of MRPS2 did not exhibit any negative effect on mitochondrial translation or OXPHOS assembly, as

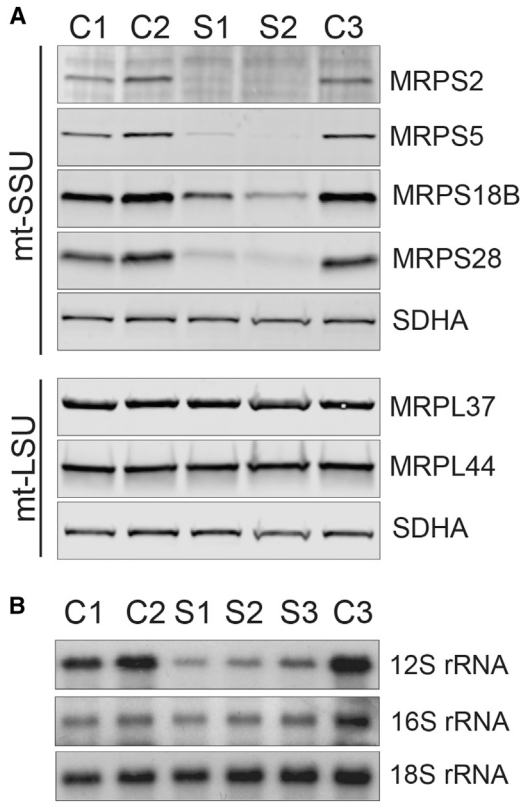

Figure 3. Abundance of mtDNA-Encoded rRNAs and Mitoribosomal Subunits

(A) SDS-PAGE analysis of proteins from the small (MRPS2, MRPS5, MRPS18B, and MRPS28) and large (MRPL37 and MRPL44) mitoribosomal subunits in both subjects and control cells revealed decreased steady-state levels of MRPS2 and the other mt-SSU proteins. Steady-state levels of the mt-LSU proteins are unaffected. OXPHOS complex II protein SDHA was used as a loading control. (B) Northern blot analysis of the steady-state levels of 12S and 16S rRNA in fibroblasts from subjects and controls demonstrates that 12S rRNA, but not 16S rRNA, is decreased in fibroblasts carrying mutations in *MRPS2* (S1 and S2) or *MRPS22* (S3). 18S rRNA from the cytosolic ribosome was used as a loading control.

evidenced by the fact that these processes were unaffected in control cells overexpressing MRPS2. Cumulatively, our complementation experiments confirm the pathogenicity of *MRPS2* mutations.

The cases presented here extend the genotypic and phenotypic spectra of mitochondrial translation deficiencies. Although all reported MRP variations invariably lead to combined OXPHOS deficiencies, their clinical presentations and prognoses are in some cases markedly different (Table 1). Defects in three proteins of mt-SSU, MRPS16,[11] MRPS22,[9,13,19] and MRPS34,[12] are reported to result in a phenotype with early lethality: four of the six subjects died in the first month of life and had a severe lactate acidemia, cardiomyopathy (except for one MRPS22-deficient subject[9]), and multi-organ failure.

Two (out of six) of the subjects with mutations in *MRPS34* did not have cardiac involvement but died in infancy from respiratory failure. The four siblings with *MRPL3* mutations also have a cardiomyopathy, but this defect seems to have a better prognosis: two siblings have survived into the second year of life, and the other two are alive at the age of 3.[8] In one of the subjects with a MRPL44 defect the cardiomyopathy was diagnosed at the age of 3 years. At 8 years old, she has a moderate non-obstructive hypertrophic cardiomyopathy.[10]

The subjects presented in this paper are at the less severe end of the clinical spectrum, and at the age of 11 years, neither shows progressive disease, despite the profound decrease in mitoribosomal assembly and OXPHOS enzyme activity detected in fibroblast cultures from these subjects. These divergent clinical presentations are inconsistent with the ubiquitous expression and seemingly equivalent roles of the mutated proteins in mitoribosomal function.

The explanation for the clinical variability in subjects with mutations in a mitochondrial ribosomal protein is likely to reside at the intersection between the different effect of each mutation on the stability or activity of the affected protein and the relative role of the different subunits in the mitoribosomal structure and assembly process. Examination of the structure of the human mt-SSU[6,7] revealed that, indeed, the three proteins for which variants lead to early lethality and that are components of the stable ~300 kDa subassembly (MRPS16, MRPS22, and MRPS34) are in close contact with each other and form a common subdomain. This subdomain is clearly separated from the other disease-implicated MRPS proteins (Figure 7A). Part of the explanation of the diverse clinical phenotypes seen in subjects with *MRPS* or *MRPL* mutations could also lie in the effects different mutations have on the stability, activity, or interactions of the mutant proteins. For example, the mutations identified in the MRPS16[11] -deficient subjects are nonsense mutations, resulting in the loss of MRPS16's mitochondrial-specific elongation extension that connects the protein to MRPS26 and MRPS30[7] and thereby disturbing its putative assembly function.[6,7] To date, almost all identified *MRPS* or *MRPL* mutations have been found to lead to moderate or severe depletion of the affected proteins. Because most mutations in mitoribosomal subunits are not complete loss-of-function alleles, they will have different effects on protein folding, stability, or activity, which might result in different residual levels of (semi)functional mitoribosomes in different tissues. Because of the different thresholds at which individual tissues are affected by diminished energy supply, this will lead to differences in tissue involvement between different mutations in mitochondrial ribosomal protein-encoding genes.

Another factor that might contribute to the differences in clinical presentation of subjects with mutations in *MRPL* or *MRPS* might be the hypothesis that destabilizing variants in subunits that join the mt-SSU or mt-LSU at an early assembly stage (as opposed to mutations in proteins that assemble later during mitoribosomal biogenesis) might lead to a more profound metabolic disturbance. Despite recent advances in elucidating the structure of the mammalian mitoribosome,[3] the order of steps in the

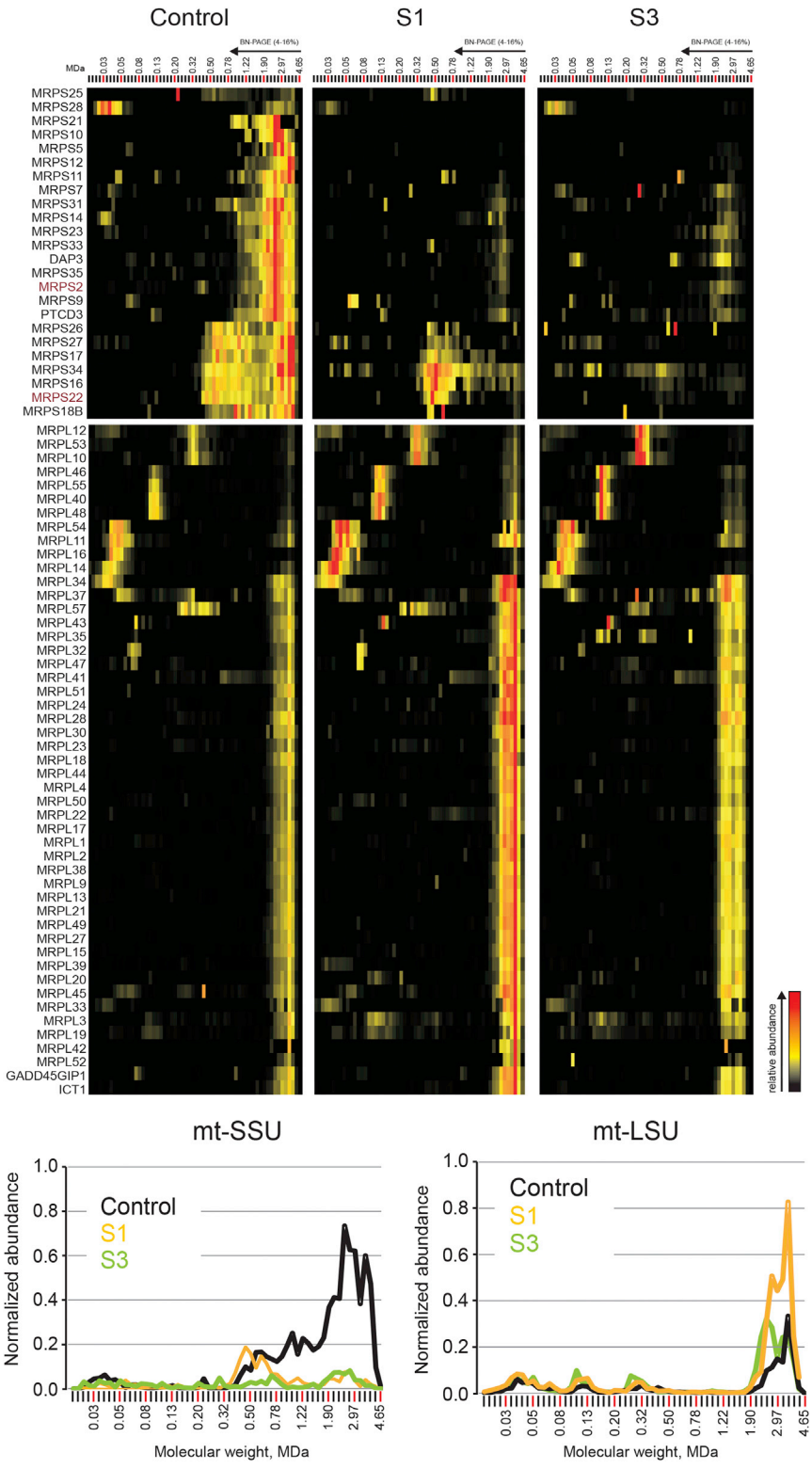

Figure 4. Complexome Profiling
Heatmap representation (top) of the migration profiles of mt-SSU and mt-LSU in control, S1, and S3 fibroblasts. Interaction heatmaps were created by hierarchical clustering, including the manual addition of known ribosomal components that were not grouped together by the algorithm. Top-center and top-right panels show decreased amounts of fully assembled mt-SSU in both S1 and S3 fibroblasts and a subassembly of eight subunits present in control and S1 cells but absent in S3 cells. The abundance of mt-LSU is unaffected in S1 and S3. Migration profiles (bottom) of both mitoribosomal subunits show the relative abundance of proteins plotted against their apparent molecular mass and reveal decreased abundance of mt-SSU and unaffected abundance of mt-LSU in both subjects. The relative abundance was calculated as the average of the normalized iBAQ values for all mt-SSU or mt-LSU proteins.

assembly process of the mitochondrial ribosome remains elusive.

MRPS2 is an evolutionary conserved protein, which suggests that it plays an important but currently unclear role in mitoribosomal biogenesis or function. The bacterial ortholog of MRPS2, bS2, is a dual-function protein. It is important for the translation of mRNAs that contain a Shine-Dalgarno sequence, a purine-rich sequence upstream of the start codon that plays an important role in the binding of the mRNA to the ribosomal RNA. BS2 recruits the bS1 ribosomal protein to bacterial SSU and stabilizes the mRNA's Shine-Dalgarno sequence during translation initiation.[20,21] In addition, bS2 plays a role in the autogenous control of bacterial ribosomal assembly as a regulator of the S2-EF-Ts operon (rpsB-tsf).[22]

BS2 is among the last proteins to assemble in the SSU particle, and because it is only loosely associated with the particle, it can be easily exchanged between subunits.[23] Mammalian MRPS2 shares a central region of orthology with bS2, but in addition it has evolved mitochondria-specific N- and C-terminal extensions, as have many other mitoribosomal proteins that are conserved in bacteria.

MRPS2 spans all three domains of the mt-SSU[6,7] and interacts with seven other mt-SSU proteins: MRPS5, MRPS9, MRPS23, MRPS28 (bS1m), MRPS18C, MRPS21, and MRPS37[2] (Figure 7A). This extended range of interactors suggests that MRPS2 has adopted a primarily structural role, which is consistent with our findings that its loss is associated with impaired mt-SSU assembly.

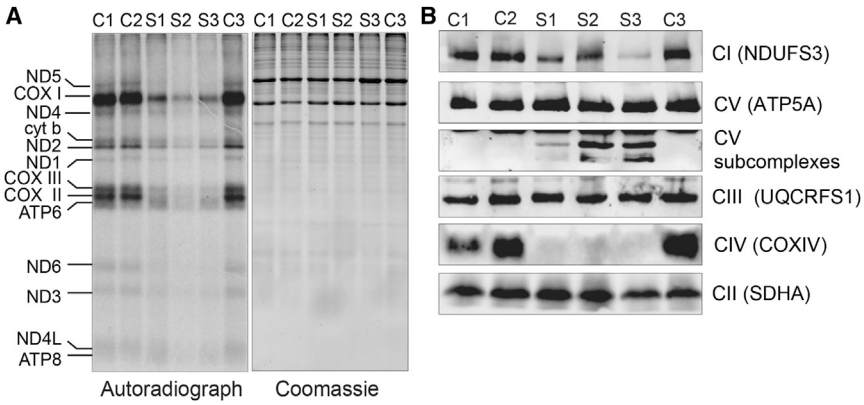

Figure 5. Pulse Labeling of Mitochondrial Translation Products and OXPHOS Assembly Analysis
(A) Pulse labeling of mitochondrial translation products in control (C1–C3), S1, S2, and S3 fibroblasts shows decreased mitochondrial protein synthesis in all subjects' cell lines. Coomassie staining of the gels was used for the assessment of loading.
(B) BN-PAGE analysis of OXPHOS assembly in control, S1, S2, and S3 fibroblasts shows decreased amounts of fully assembled OXPHOS complexes I and IV in the fibroblasts from the MRPS2- and MRPS22-deficient subjects. Subcomplexes of complex V accumulate in subjects' fibroblasts and are absent in the control cells.

Although MRPS2 interacts with MRPS5 and MRPS28, which are involved in mRNA recruitment and exit from the mitoribosome, respectively, the role of MRPS2 in translation has most likely been lost in evolution. Mitochondrial mRNAs do not have Shine-Dalgarno sequences. Bacterial bS2 is dispensable for the translation of mRNAs without such a sequence, and this could be the case for MRPS2 in mitochondria as well. In summary, our data support a structural role for MRPS2 in the connection of different domains of the mitochondrial ribosome.

We propose that MRPS2, like bS2 and consistent with our complexome profiling data (Figure 4) and the structure of mtSSU (Figure 7A), most likely assembles late in mitoribosomal biogenesis and that this assembly is probably independent of the set of core proteins, which include MRPS22 and MRPS16, forming the ~300 kDa subassembly. Notably, after depletion of these subunits in subjects with mutations in the encoding genes, large amounts of MRPS2 and mt-LSU were still detectable.[24] This late assembly might explain the less severe phenotype in our subjects.

A more detailed inspection of the position of the affected residues within MRPS2 (Figure 7B) showed that the two residues that were altered in S1 are found in a region that faces the 12S RNA and tightly interacts with several other proteins. In contrast, the arginine exchanged in S2 is

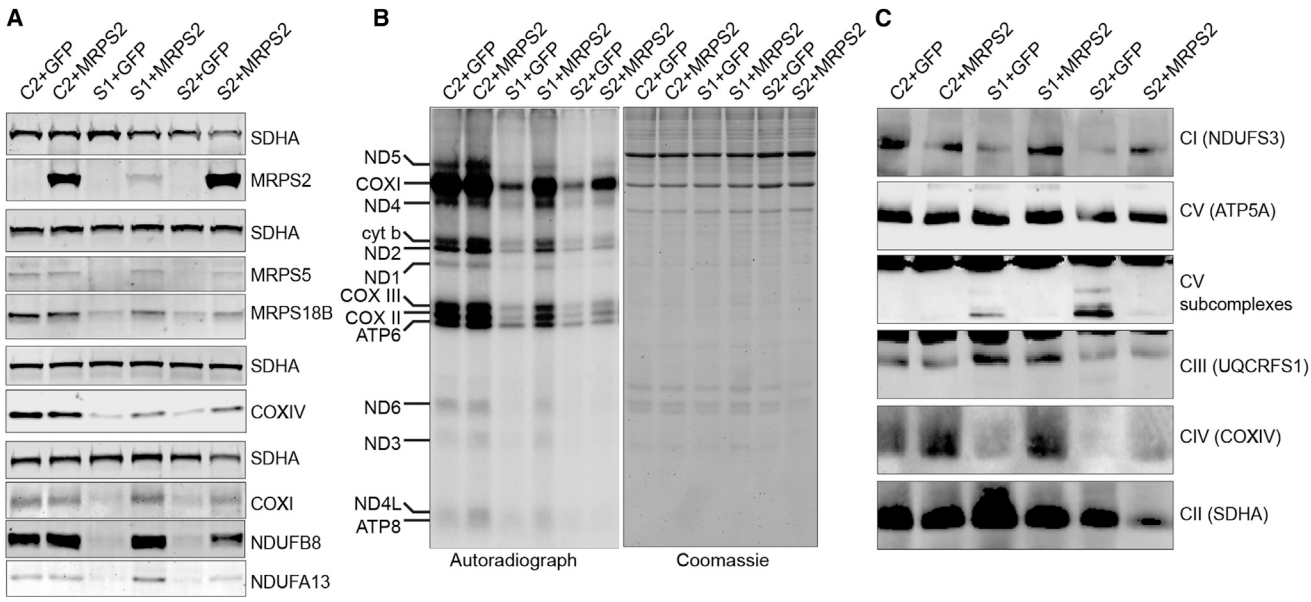

Figure 6. Amounts of Wild-Type MRPS2 in S1 and S2 Fibroblasts
(A) Immunoblot analysis of whole-cell extracts from control (C), S1, and S2 cell lines transduced with a lentivirus expressing either wild-type MRPS2 (+MRPS2) or green fluorescent protein (+GFP) as a negative control. The presence of wild-type MRPS2 leads to increased amounts of MRPS5 and MRPS18B, as well as NDUFB8 and NDUFA13 from complex I and COXI and COXIV from complex IV. MRPS2 was detected with a specific antiserum that does not detect the endogenous MRPS2 in whole-cell extracts. SDHA was used as a loading control for each separate gel.
(B) Pulse labeling of mitochondrial translation products demonstrates that the presence of wild-type MRPS2 partially restores mitochondrial translation in S1 and S2 fibroblasts. The gel was stained with Coomassie colloidal dye for the assessment of loading.
(C) BN-PAGE analysis of OXPHOS assembly in C, S1, and S2 fibroblasts transfected with either GFP- or wild-type-MRPS2-expressing lentivirus shows partial restoration of OXPHOS complex assembly in subject cells expressing MRPS2.

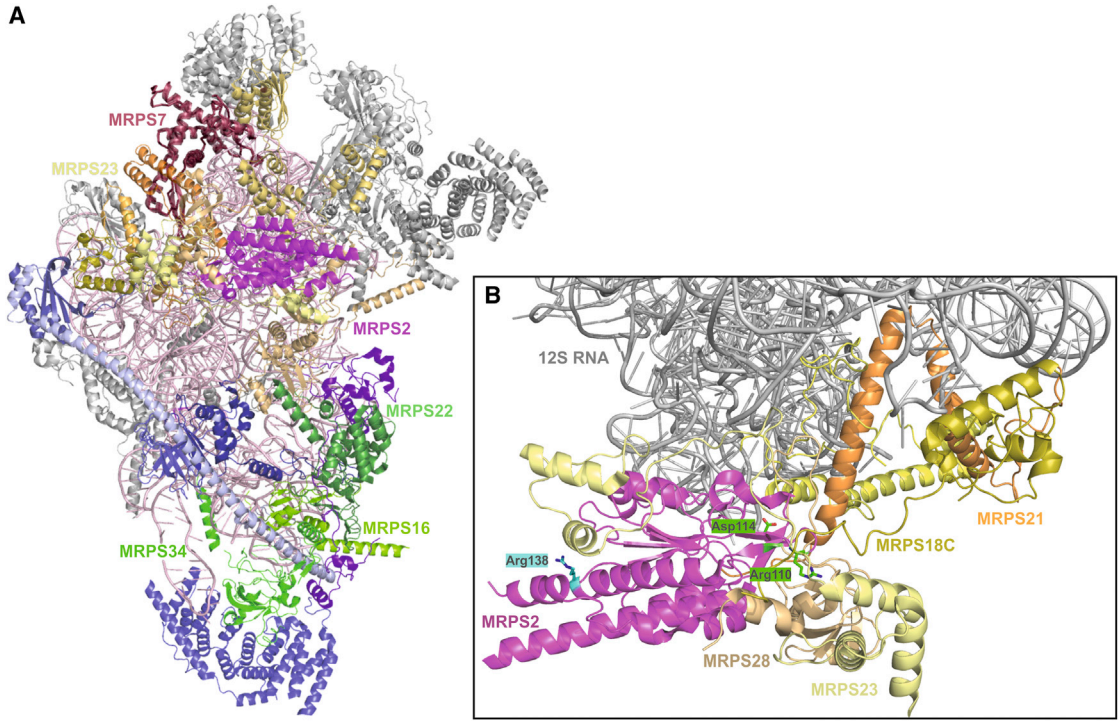

Figure 7. Structural Model of the Human mt-SSU Shows the Positions of Affected Proteins and Residues
(A) The human 28S mt-SSU (PDB: 3J9M[7]) was drawn in cartoon representation with PyMol version 1.7.4.0. The subunits known to be implicated in disease are shown with color-matched labels: magenta, MRPS2; raspberry, MRPS7; pale yellow, MRPS23; and shades of green, MPRS16, MRPS22, and MRPS34. Subunits interacting with MRPS2 are shown in shades of yellow, and constituents of the ~300 kDa subassembly are shown in shades of blue and green. Other subunits are shown in gray, and 12S RNA is shown in light pink. (B) Partial model of (A) shows only the 12S RNA (gray), MRPS2 (magenta), and surrounding proteins MRPS18C, MRPS21, and MRPS28 (shades of yellow). The positions of the residues of MRPS2 altered in S1 (Arg110 and Asp114) and in S3 (Arg138) are shown in green and cyan, respectively, as stick models.

located near the surface of mt-SSU, suggesting more indirect effects on the stability of the complex. This difference might also explain why the amount of 12S RNA found in S1 was slightly lower than in S2 (Figure 3B).

A distinctive clinical feature in subject 1 was wrinkly skin. To date, dermatological symptoms in subjects with mutations in MRP genes have been limited to redundant skin of the neck, which was previously described in single subjects carrying either *MRPS22* or *MRPS16* mutations.[9,11,13] However, disturbed mitochondrial metabolism has been previously linked to wrinkled skin in association with progeria[25–27] and in subjects carrying *PYCR1* (MIM: 179035) and *ALDH18A1* (also known as *P5CS*) (involved in *de novo* proline synthesis) mutations leading to multisystemic disorders with cutis laxa, a typical facial gestalt, hypotonia, and intellectual disability.[25–28] Of note, although metabolic markers (blood lactate and alanine elevation) of mitochondrial disease have been found in one subject with PYCR1 deficiency,[25] OXPHOS activities and lactate levels are typically normal in these subjects, which sets them apart from those carrying MRP alterations. Moreover, hearing impairment is very rare in cutis laxa or wrinkly skin syndromes; it has only been described as an incidental finding in studies of P5CS deficiency, which makes this wrinkly-skin syndrome recognizable.[29–32]

Together, our data demonstrate that mutations in *MRPS2*, which encodes a mitoribosomal protein, cause a recognizable phenotype involving sensorineural deafness, hypoglycemia, lactic acidemia, 2-oxoglutaric aciduria, developmental delay, and multiple-OXPHOS-complex dysfunction. Especially in the presence of wrinkled skin, these are discriminative features that, when encountered, should raise suspicion for a MRP-related mitochondrial defect. The clinical recognition of these features should allow a targeted diagnostic approach to MRP deficiencies.

Supplemental Data

Supplemental Data include Supplemental Material and Methods, one figure, and one table and can be found with this article online at https://doi.org/10.1016/j.ajhg.2018.02.012.

Acknowledgments

We thank the subjects and their parents for their participation. This study was financially supported by the Dutch Metakids foundation (2012, M.M.), the Netherlands Organisation for Scientific Research (2011, NWO project 017.008.052, M.M.), the E-Rare project GENOMIT (01GM1207, A.R.), the National Institutes of Health (HL090648, Z.U.), and the Association Français contre les Myopathies (19876, M.D.M). B.R., A.R., and M.D.M would like to acknowledge the technical assistance with cell

culture from Ms. Coralie Zangarelli. Exome sequencing of subject 2 was done in collaboration with the Centre National de Génotypage.

Received: October 31, 2017
Accepted: February 19, 2018
Published: March 22, 2018

Web Resources

GenBank, https://www.ncbi.nlm.nih.gov/genbank/
gnomAD Browser, http://gnomad.broadinstitute.org
MITOMAP, http://www.mitomap.org/mitomap
OMIM, http://www.omim.org/
PDB, http://www.rcsb.org/
PolyPhen-2, http://genetics.bwh.harvard.edu/pph2/
SIFT, http://sift.jcvi.org

References

1. Pearce, S., Nezich, C.L., and Spinazzola, A. (2013). Mitochondrial diseases: translation matters. Mol. Cell. Neurosci. *55*, 1–12.
2. Amunts, A., Brown, A., Toots, J., Scheres, S.H.W., and Ramakrishnan, V. (2015). Ribosome. The structure of the human mitochondrial ribosome. Science *348*, 95–98.
3. Greber, B.J., Boehringer, D., Leibundgut, M., Bieri, P., Leitner, A., Schmitz, N., Aebersold, R., and Ban, N. (2014). The complete structure of the large subunit of the mammalian mitochondrial ribosome. Nature *515*, 283–286.
4. Greber, B.J., Boehringer, D., Leitner, A., Bieri, P., Voigts-Hoffmann, F., Erzberger, J.P., Leibundgut, M., Aebersold, R., and Ban, N. (2014). Architecture of the large subunit of the mammalian mitochondrial ribosome. Nature *505*, 515–519.
5. Rorbach, J., Gao, F., Powell, C.A., D'Souza, A., Lightowlers, R.N., Minczuk, M., and Chrzanowska-Lightowlers, Z.M. (2016). Human mitochondrial ribosomes can switch their structural RNA composition. Proc. Natl. Acad. Sci. USA *113*, 12198–12201.
6. Kaushal, P.S., Sharma, M.R., Booth, T.M., Haque, E.M., Tung, C.S., Sanbonmatsu, K.Y., Spremulli, L.L., and Agrawal, R.K. (2014). Cryo-EM structure of the small subunit of the mammalian mitochondrial ribosome. Proc. Natl. Acad. Sci. USA *111*, 7284–7289.
7. Kaushal, P.S., Sharma, M.R., Booth, T.M., Haque, E.M., Tung, C.S., Sanbonmatsu, K.Y., Spremulli, L.L., and Agrawal, R.K. (2014). Cryo-EM structure of the small subunit of the mammalian mitochondrial ribosome. Proc. Natl. Acad. Sci. USA *111*, 7284–7289.
8. Galmiche, L., Serre, V., Beinat, M., Assouline, Z., Lebre, A.S., Chretien, D., Nietschke, P., Benes, V., Boddaert, N., Sidi, D., et al. (2011). Exome sequencing identifies MRPL3 mutation in mitochondrial cardiomyopathy. Hum. Mutat. *32*, 1225–1231.
9. Smits, P., Saada, A., Wortmann, S.B., Heister, A.J., Brink, M., Pfundt, R., Miller, C., Haas, D., Hantschmann, R., Rodenburg, R.J., et al. (2011). Mutation in mitochondrial ribosomal protein MRPS22 leads to Cornelia de Lange-like phenotype, brain abnormalities and hypertrophic cardiomyopathy. Eur. J. Hum. Genet. *19*, 394–399.
10. Distelmaier, F., Haack, T.B., Catarino, C.B., Gallenmüller, C., Rodenburg, R.J., Strom, T.M., Baertling, F., Meitinger, T., Mayatepek, E., Prokisch, H., and Klopstock, T. (2015). MRPL44 mutations cause a slowly progressive multisystem disease with childhood-onset hypertrophic cardiomyopathy. Neurogenetics *16*, 319–323.
11. Miller, C., Saada, A., Shaul, N., Shabtai, N., Ben-Shalom, E., Shaag, A., Hershkovitz, E., and Elpeleg, O. (2004). Defective mitochondrial translation caused by a ribosomal protein (MRPS16) mutation. Ann. Neurol. *56*, 734–738.
12. Lake, N.J., Webb, B.D., Stroud, D.A., Richman, T.R., Ruzzenente, B., Compton, A.G., Mountford, H.S., Pulman, J., Zangarelli, C., Rio, M., et al. (2017). Biallelic Mutations in MRPS34 Lead to Instability of the Small Mitoribosomal Subunit and Leigh Syndrome. Am. J. Hum. Genet. *101*, 239–254.
13. Saada, A., Shaag, A., Arnon, S., Dolfin, T., Miller, C., Fuchs-Telem, D., Lombes, A., and Elpeleg, O. (2007). Antenatal mitochondrial disease caused by mitochondrial ribosomal protein (MRPS22) mutation. J. Med. Genet. *44*, 784–786.
14. Kohda, M., Tokuzawa, Y., Kishita, Y., Nyuzuki, H., Moriyama, Y., Mizuno, Y., Hirata, T., Yatsuka, Y., Yamashita-Sugahara, Y., Nakachi, Y., et al. (2016). A Comprehensive Genomic Analysis Reveals the Genetic Landscape of Mitochondrial Respiratory Chain Complex Deficiencies. PLoS Genet. *12*, e1005679.
15. Gilissen, C., Arts, H.H., Hoischen, A., Spruijt, L., Mans, D.A., Arts, P., van Lier, B., Steehouwer, M., van Reeuwijk, J., Kant, S.G., et al. (2010). Exome sequencing identifies WDR35 variants involved in Sensenbrenner syndrome. Am. J. Hum. Genet. *87*, 418–423.
16. Menezes, M.J., Guo, Y., Zhang, J., Riley, L.G., Cooper, S.T., Thorburn, D.R., Li, J., Dong, D., Li, Z., Glessner, J., et al. (2015). Mutation in mitochondrial ribosomal protein S7 (MRPS7) causes congenital sensorineural deafness, progressive hepatic and renal failure and lactic acidemia. Hum. Mol. Genet. *24*, 2297–2307.
17. Heide, H., Bleier, L., Steger, M., Ackermann, J., Dröse, S., Schwamb, B., Zörnig, M., Reichert, A.S., Koch, I., Wittig, I., and Brandt, U. (2012). Complexome profiling identifies TMEM126B as a component of the mitochondrial complex I assembly complex. Cell Metab. *16*, 538–549.
18. Wessels, H.J., Vogel, R.O., Lightowlers, R.N., Spelbrink, J.N., Rodenburg, R.J., van den Heuvel, L.P., van Gool, A.J., Gloerich, J., Smeitink, J.A., and Nijtmans, L.G. (2013). Analysis of 953 human proteins from a mitochondrial HEK293 fraction by complexome profiling. PLoS ONE *8*, e68340.
19. Baertling, F., Haack, T.B., Rodenburg, R.J., Schaper, J., Seibt, A., Strom, T.M., Meitinger, T., Mayatepek, E., Hadzik, B., Selcan, G., et al. (2015). MRPS22 mutation causes fatal neonatal lactic acidosis with brain and heart abnormalities. Neurogenetics *16*, 237–240.
20. Kaminishi, T., Wilson, D.N., Takemoto, C., Harms, J.M., Kawazoe, M., Schluenzen, F., Hanawa-Suetsugu, K., Shirouzu, M., Fucini, P., and Yokoyama, S. (2007). A snapshot of the 30S ribosomal subunit capturing mRNA via the Shine-Dalgarno interaction. Structure *15*, 289–297.
21. Laughrea, M., and Moore, P.B. (1978). Ribosomal components required for binding protein S1 to the 30 S subunit of Escherichia coli. J. Mol. Biol. *122*, 109–112.

22. Aseev, L.V., Levandovskaya, A.A., Tchufistova, L.S., Scaptsova, N.V., and Boni, I.V. (2008). A new regulatory circuit in ribosomal protein operons: S2-mediated control of the rpsB-tsf expression in vivo. RNA *14*, 1882–1894.
23. Brodersen, D.E., Clemons, W.M., Jr., Carter, A.P., Wimberly, B.T., and Ramakrishnan, V. (2002). Crystal structure of the 30 S ribosomal subunit from Thermus thermophilus: structure of the proteins and their interactions with 16 S RNA. J. Mol. Biol. *316*, 725–768.
24. Emdadul Haque, M., Grasso, D., Miller, C., Spremulli, L.L., and Saada, A. (2008). The effect of mutated mitochondrial ribosomal proteins S16 and S22 on the assembly of the small and large ribosomal subunits in human mitochondria. Mitochondrion *8*, 254–261.
25. Dimopoulou, A., Fischer, B., Gardeitchik, T., Schröter, P., Kayserili, H., Schlack, C., Li, Y., Brum, J.M., Barisic, I., Castori, M., et al. (2013). Genotype-phenotype spectrum of PYCR1-related autosomal recessive cutis laxa. Mol. Genet. Metab. *110*, 352–361.
26. Reversade, B., Escande-Beillard, N., Dimopoulou, A., Fischer, B., Chng, S.C., Li, Y., Shboul, M., Tham, P.Y., Kayserili, H., Al-Gazali, L., et al. (2009). Mutations in PYCR1 cause cutis laxa with progeroid features. Nat. Genet. *41*, 1016–1021.
27. Bicknell, L.S., Pitt, J., Aftimos, S., Ramadas, R., Maw, M.A., and Robertson, S.P. (2008). A missense mutation in ALDH18A1, encoding Delta1-pyrroline-5-carboxylate synthase (P5CS), causes an autosomal recessive neurocutaneous syndrome. Eur. J. Hum. Genet. *16*, 1176–1186.
28. Wolthuis, D.F., van Asbeck, E., Mohamed, M., Gardeitchik, T., Lim-Melia, E.R., Wevers, R.A., and Morava, E. (2014). Cutis laxa, fat pads and retinopathy due to ALDH18A1 mutation and review of the literature. European journal of paediatric neurology *18*, 511–515.
29. Berk, D.R., Bentley, D.D., Bayliss, S.J., Lind, A., and Urban, Z. (2012). Cutis laxa: a review. J. Am. Acad. Dermatol. *66*, 1–17.
30. Morava, E., Guillard, M., Lefeber, D.J., and Wevers, R.A. (2009). Autosomal recessive cutis laxa syndrome revisited. Eur. J. Hum. Genet. *17*, 1099–1110.
31. Gardeitchik, T., Mohamed, M., Fischer, B., Lammens, M., Lefeber, D., Lace, B., Parker, M., Kim, K.J., Lim, B.C., Häberle, J., et al. (2014). Clinical and biochemical features guiding the diagnostics in neurometabolic cutis laxa. Eur. J. Hum. Genet. *22*, 888–895.
32. Mohamed, M., Kouwenberg, D., Gardeitchik, T., Kornak, U., Wevers, R.A., and Morava, E. (2011). Metabolic cutis laxa syndromes. J. Inherit. Metab. Dis. *34*, 907–916.
33. Serre, V., Rozanska, A., Beinat, M., Chretien, D., Boddaert, N., Munnich, A., Rötig, A., and Chrzanowska-Lightowlers, Z.M. (2013). Mutations in mitochondrial ribosomal protein MRPL12 leads to growth retardation, neurological deterioration and mitochondrial translation deficiency. Biochim. Biophys. Acta *1832*, 1304–1312.

The American Journal of Human Genetics, Volume *102*

Supplemental Data

Bi-allelic Mutations in the Mitochondrial Ribosomal Protein MRPS2 Cause Sensorineural Hearing Loss, Hypoglycemia, and Multiple OXPHOS Complex Deficiencies

Thatjana Gardeitchik, Miski Mohamed, Benedetta Ruzzenente, Daniela Karall, Sergio Guerrero-Castillo, Daisy Dalloyaux, Mariël van den Brand, Sanne van Kraaij, Ellyze van Asbeck, Zahra Assouline, Marlene Rio, Pascale de Lonlay, Sabine Scholl-Buergi, David F.G.J. Wolthuis, Alexander Hoischen, Richard J. Rodenburg, Wolfgang Sperl, Zsolt Urban, Ulrich Brandt, Johannes A. Mayr, Sunnie Wong, Arjan P.M. de Brouwer, Leo Nijtmans, Arnold Munnich, Agnès Rötig, Ron A. Wevers, Metodi D. Metodiev, and Eva Morava

Supplemental Material and Methods

Whole exome sequencing

Whole-exome sequencing (WES) was performed on genomic DNA extracted from patient lymphocytes using standard salting out methods on two different platforms. Details on exome capture and sequencing are available upon request. Potential pathogenicity of the identified genetic variations was evaluated using literature, evolutionary conservation, SIFT (http://sift.jcvi.org) and PolyPhen 2 (http://genetics.bwh.harvard.edu/pph2/). Earlier reporting of identified genetic variations was checked using data from our in house database and the Genome Aggregation Consortium, gnomAD (Cambridge, MA; http://gnomad.broadinstitue.org). All databases were accessed July 2017. Sequence validation and segregation analysis of the candidate variants were performed with Sanger sequencing (reference sequences GenBank: M_016034.3]). Variant nomenclature adheres to the Human Genome Variation Society (HGVS) guidelines.

Northern blot analysis

RNA for Northern blot analysis was extracted from cells grown in 25cm^2 flasks using Trizol (Thermo Fisher Scientific, Courtaboeuf, France). 1 μg RNA was fractionated through 1.2% Agarose gel and transferred onto a Nylon membrane (Merck Millipore, Fontenay sous Bois, France) using capillary transfer. After UV crosslinking, the membrane was blocked at 55^{o}C with blocking buffer (Sigma Aldrich, Lyon, France). To generate specific DNA probes against 12S, 16S and 18S rRNA, we cloned the corresponding PCR-amplified DNA fragments into pCRII-TOPO vector (Thermo Fisher Scientific Courtabeuf, France). Prior to labeling, the DNA constructs were digested with EcoRI restriction enzyme and the fragments were gel-purified. Purified DNA (50 ng) probe was radiolabeled using the Random Primers DNA Labeling System (Thermo Fisher Scientific Courtabeuf, France) and 50 μCi of [α-^{32} P]-dCTP. Membranes were incubated with the probes for at least 2 hours at 55^{o}C followed by washing with 2xSSC-0.1%SDS buffer at room temperature. Membranes were exposed to Hyperfilm MP multipurpose films (GE Healthcare, Succursale, France) at room temperature for at least 1 hr.

SDS-PAGE and immunodetection

Samples for SDS-PAGE were prepared either from isolated mitochondria or whole-cell extracts. Mitochondria, isolated as described previously [1], were recentrifuged at 12,000 g for

10 min in a cooled benchtop centrifuge, and pellets were resuspended in SDS PAGE sample loading buffer at concentration of 2 μg/μl. 30 μg were fractionated through 12% Mini-Protean TGX precast gels and transferred onto low fluorescent PVDF membranes (Bio-Rad, Marnes-la Coquette, France). Mitoribosomal proteins were detected using the following specific antisera: anti-MRPS2 (Abcam, Paris, France), anti-MRPS18B (Proteintech Europe, Manchester, UK), anti-MRPS5 (Abcam, Paris, France), anti-MRPS28 (Proteintech Europe, Manchester, UK), anti-MRPL37 (Sigma-Aldrich, Lyon, France) and anti-MRPL44 (Proteintech Europe, Manchester, UK). Anti-SDHA, used as a loading control was from Abcam.

Whole-cell extracts were prepared as described in Analysis of Mitochondrial Translation. 20 μg were fractionated as above, transferred on PVDF membranes and probed with some of the specific antisera mentioned above and in addition: anti-NDUFB8 (Abcam, Paris, France), NDUFA13 (Abcam, Paris, France), anti-COXIV (Proteintech Europe, Manchester, UK) and anti-COXI (MTCO1, Abcam, Paris, France).

IR Dye-conjugated, anti-mouse (780 nm) or anti-rabbit (680 nm) secondary antibodies were used at a dilution of 1:5000 and were purchased from Li-Cor Biosciences (Bad Homburg, Germany). Membranes were scanned with Odyssey CLX infrared scanner.

BN-PAGE and immunodetection

Isolation of mitochondria and Blue native gradient (5%–15%) gel electrophoresis (BN-PAGE) were performed as described previously by Calvaruso, et al. [2] Lanes were loaded with equal amounts of solubilized (mitochondrial) protein (80 or 120 μg). Gels were blotted to nitrocellulose transfer membranes (Whatman, ‘s-Hertogenbosch, the Netherlands). Membranes were incubated with the following specific antibodies: mouse anti-NDUFS3 (Invitrogen, Leek, the Netherlands), mouse anti-SDHA (Mitosciences, Eugene, USA), mouse anti-UQCRFS1 (Proteintech, Rosemont, USA), mouse anti-COXIV(Mitosciences, Eugene, USA)) and mouse anti-ATP5A (Abcam, Cambridge, UK). Goat anti-(mouse Ig) Ig peroxidase (1:10,000; GAMPO; Invitrogen, Leek, the Netherlands) was used as a secondary antibody for detection. Signal was generated using the ECL Prime Western Blotting reagent (Biosciences, Roosendaal, the Netherlands).

Analysis of mitochondrial protein synthesis

In vitro pulse labeling of mitochondrial translation products was performed essentially as described before [3]. Briefly, near-confluent fibroblasts were incubated for 30 minutes at 37 °C

in methionine- and cysteine-free DMEM media (Thermo Fisher Scientific, Courtaboeuf, France) supplemented with dialyzed FBS (Thermo Fisher Scientific, Courtaboeuf, France) and 400 μCi of EasyTag Express35S protein labeling mix (Perkin Elmer SAS, Cortaboeuf, France) in the presence of 100μg/ml of the cytosolic translation inhibitor emetine. At the end of the pulse, labelling media was substituted with standard DMEM growth media followed by a 10 min incubation during which synthesis of labelled translation products is completed. Cells were washed twice with ice-cold PBS (Thermo Fisher Scientific, Courtaboeuf, France) and harvested by scraping in 1ml PBS. Cells were reisolated by centrifugation at 2000xg for 10min in a cooled centrifuge and resuspended in 50 μl PBS. Bradford assay (Sigma-Aldrich, Lyon, France) was performed on the cell suspensions, which were then centrifuged as before and cell pellets were resuspended in 2x SDS PAGE loading buffer at a concentration of 1μg/μl. 10 μg of each sample were fractionated through a 17% SDS polyacrylamide gel (Protean II XL, Bio-Rad, Marnes-la Coquette, France) for overnight at 110V. The gel was stained with Coomassie blue colloidal dye and incubated for 20 min in Amplify fluorographic reagent (GE Healthcare, Succursale, France) prior to drying. Exposures were for up to 5 days at -80^{o}C using Hyperfilm MP multipurpose films (GE Healthcare, Succursale, France).

Complexome profiling

In-gel tryptic digestion, mass spectrometry and data analysis were performed as described by Huynen, et al[7]. In summary a mitochondrial enriched fraction of solubilized protein was loaded on a blue native gradient gel. Lanes were sliced into 60 even pieces, proteins were digested with trypsin. Peptides were extracted and analyzed by liquid chromatography tandem mass spectrometry (LC-MS/MS) in a Q-exactive mass spectrometer (Thermo Fisher Scientific, Whalthma, MA, USA). All raw files were analyzed by MaxQuant software (version 1.4.1.2[8]). Unique plus razor peptides were considered for protein quantification. Protein abundance migration profiles were normalized considering multiple profiles, that is, taking into account iBAQ values from all slices. Profiles were hierarchically clustered using Cluster 3.0 software [9,10] by distance measures based on Pearson correlation coefficient (uncentered) and the average linkage method.

Cloning of human MRPS2 and lentiviral transduction

Wild type MRPS2 was amplified from cDNA using primers designed according to the recommendations for cloning using the Electra cloning technology (Atum, Basel, Switzerland): Forward primer: 5'- TACACGTACTTAGTCGCTGAAGCTCTTCT**ATGGC**

GACATCCTCGGCC–3’ and reverse primer: AGGTACGAACTCGATTGACGGCTCTTC TACC**TCACAGGGAATGGCTCATGTCA**-3’; the sequence complementary to the MRPS2 cDNA is indicated in bold) and cloned in a lentiviral vector pD2109-CMV (Atum, Basel, Switzerland) carrying a puromycin resistance gene, which enables the generation of stably transduced cell lines. The corresponding control vector pD2109-CMV-03 expressing GFP was also purchased from Atum. Production of lentiviral particles was performed in HEK293FT cells transfected with either of the above lentiviruses and viral packaging constructs expressing REV, VSV-G and PAX2. Cells were incubated for 72 hours and culture supernatants were collected, filtered through 0.2 μm sterile filters and used for transduction of near confluent control and patient fibroblasts. Puromycin (Thermo Fisher Scientific, Courtaboeuf, France) was added 72 hours after transduction at a final concentration of 3 μg/ml and selection was performed for 2 weeks during which media was changed every two days. Under these conditions, about 10-20% of the initially transduced cells survived the puromycin selection. At the end of this procedure, surviving cells carry stably integrated MRPS2- or GFP-expressing vectors.

Web Resources

GenBank, https://www.ncbi.nlm.nih.gov/genbank/

OMIM, http://www.omim.org

MutationTaster, http://www.mutationtaster.org

PolyPhen-2, http://genetics.bwh.harvard.edu/pph2/

SIFT, http://sift.jcvi.org

Figure S1

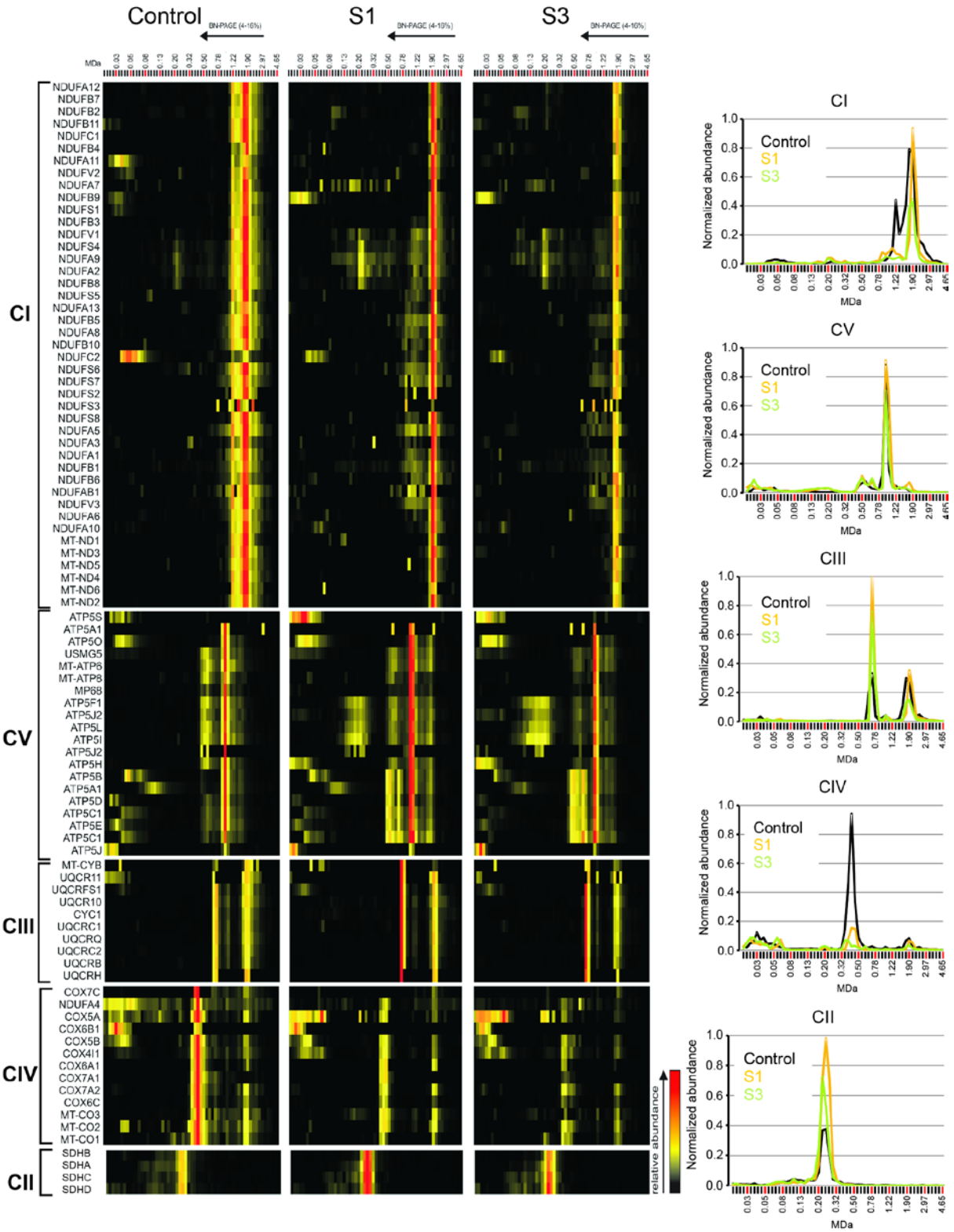

Figure S1. Complexome profiling of OXPHOS complex assembly

Heat maps (**left**) and migration profiles (**right**) of OXPHOS complexes in control, S1 and SS3 fibroblasts demonstrating defects in multiple OXPHOS Complexes and an accumulation of CI and CV assembly intermediates in both [11].

Supplementary Table 1 Identified *MRPS2* variants and predictions of their pathogenicity

	Subject 1	**Subject 1**	**Subject 2**
Nucleotide change	c.328C>T	c.340G>A	c.413G>A
Amino Acid change	p.Arg110Cys	p.Asp114Asn	p.Arg138His
SIFT	Deleterious	Tolerated	Deleterious
PolyPhen-2	Probably damaging	Probably damaging	Probably damaging
Mutation Taster	Disease causing	Disease causing	Disease causing
dbSNP	rs791334309	rs201229537	rs758539748
gnomAD allele frequency	0.00001450%	0.00008318	0.00005282

Pathogenicity was predicted by SIFT. MutationTaster. and PolyPhen-2. Earlier reporting of identified genetic variations was checked using data from the Genome Aggregation Database. gnomAD. Allele frequencies for both RefSNP numbers are not reported. The *MRPS2* reference sequence used is GenBank accession code NM_016034.3

1. Metodiev, M.D., Lesko, N., Park, C.B., Camara, Y., Shi, Y., Wibom, R., Hultenby, K., Gustafsson, C.M., and Larsson, N.G. (2009). Methylation of 12S rRNA is necessary for in vivo stability of the small subunit of the mammalian mitochondrial ribosome. Cell metabolism 9, 386-397.
2. Calvaruso, M.A., Smeitink, J., and Nijtmans, L. (2008). Electrophoresis techniques to investigate defects in oxidative phosphorylation. Methods (San Diego, Calif) 46, 281-287.
3. Sasarman, F., and Shoubridge, E.A. (2012). Radioactive labeling of mitochondrial translation products in cultured cells. Methods Mol Biol 837, 207-217.
4. Janssen, A.J., Trijbels, F.J., Sengers, R.C., Smeitink, J.A., van den Heuvel, L.P., Wintjes, L.T., Stoltenborg-Hogenkamp, B.J., and Rodenburg, R.J. (2007). Spectrophotometric assay for complex I of the respiratory chain in tissue samples and cultured fibroblasts. Clinical chemistry 53, 729-734.
5. Jonckheere, A.I., Hogeveen, M., Nijtmans, L., van den Brand, M., Janssen, A., Diepstra, H., van den Brandt, F., van den Heuvel, B., Hol, F., Hofste, T., et al. (2009). A novel mitochondrial ATP8 gene mutation in a patient with apical hypertrophic cardiomyopathy and neuropathy. BMJ case reports 2009.
6. Rodenburg, R.J. (2011). Biochemical diagnosis of mitochondrial disorders. Journal of inherited metabolic disease 34, 283-292.
7. Huynen, M.A., Muhlmeister, M., Gotthardt, K., Guerrero-Castillo, S., and Brandt, U. (2016). Evolution and structural organization of the mitochondrial contact site (MICOS) complex and the mitochondrial intermembrane space bridging (MIB) complex. Biochimica et biophysica acta 1863, 91-101.
8. Cox, J., and Mann, M. (2008). MaxQuant enables high peptide identification rates, individualized p.p.b.-range mass accuracies and proteome-wide protein quantification. Nature biotechnology 26, 1367-1372.
9. de Hoon, M.J., Imoto, S., Nolan, J., and Miyano, S. (2004). Open source clustering software. Bioinformatics (Oxford, England) 20, 1453-1454.
10. Eisen, M.B., Spellman, P.T., Brown, P.O., and Botstein, D. (1998). Cluster analysis and display of genome-wide expression patterns. Proceedings of the National Academy of Sciences of the United States of America 95, 14863-14868.

17. Heide, H., Bleier, L., Steger, M., Ackermann, J., Drose, S., Schwamb, B., Zornig, M., Reichert, A.S., Koch, I., Wittig, I., et al. (2012). Complexome profiling identifies TMEM126B as a component of the mitochondrial complex I assembly complex. Cell metabolism 16, 538-549.